

A 80-004 High-Performance Parabolic Antenna Reflectors

J. S. Archer*

TRW Defense and Space Systems Group, Redondo Beach, Calif.

The configuration of lightweight high-precision parabolic reflectors for high-performance communication spacecraft has required the development of new materials, techniques, and processes to satisfy current design specifications. Lightweight thermally stable designs dictate the use of high-performance composite materials. Thermally sensitive off-axis configurations require special attention for optimum design. The use of linear polarization with imbedded grids restricts the configuration to specific composite materials and special manufacturing processes. The development of designs with near-zero thermal expansion has required the investigation of many material properties which are usually considered secondary and consequently ignored in conventional designs. The requirement for precision contours with cost-effective processes has led to the use of postfabrication adjustment techniques as standard procedure.

Introduction

THE accommodation of antenna systems has a major influence in the external design configuration of current military and commercial communication spacecraft. The design of specific antenna configurations may be severely constrained by requirements for shroud clearance when stowed, deployment kinematics, field-of-view, rf isolation, and adequate stiffness for attitude control or pointing. The reflector arrangements on Intelsat V and TDRSS are so dominant that the antenna configuration is referred to as the "antenna farm." The multiple access antenna system on TDRSS is known as the "cornfield." One may observe without exaggeration that some spacecraft are flying antennas.

The mechanical design of high-precision antenna parabolic reflectors to meet the rapidly growing requirements of modern communication spacecraft is a major technical challenge. High data transmission rates have pushed frequencies up from a few megahertz to 60 GHz, with the attendant high-precision construction and thermoelastic performance requirements. Operations at 100 and 200 GHz are now being studied for future applications. Light weight, combined with thermal stability requirements, has led to the utilization of composite materials of construction with all the attendant process development and manufacturing control problems. Long-term space exposure thermal cycle environments has led to serious investigation of what were previously considered to be secondary effects in the materials behavior. The presence of anisotropic material properties and the utilization of off-axis reflector configurations have required the development of sophisticated analytical analyses which reflect the secondary parameters that affect the reflector performance.

This paper attempts to describe some of the design trends, analytical results, material and fabrication processes, and test

techniques which have been developed and utilized successfully over the last decade for antenna reflectors with solid surfaces (in contrast to rib-mesh configurations).

Configuration

Classically, large parabolic antenna reflectors have been designed with axisymmetric configurations, either direct-fed or with Cassegrain subreflectors. However, in order to eliminate blockage and radiation pattern disturbances, many current designs utilize off-axis configurations. The sensitivity of the off-axis design to thermal disturbances is significantly greater than that of an axisymmetric design. Electrical axis pointing and defocus can be as much as one order of magnitude larger for the off-axis case when compared to a similar symmetrical configuration.

Additional complexity in reflector designs arises with the utilization of linearly polarized beams, with the polarization provided mechanically by grids embedded in the surface of the parabolic dish. Current process developments provide for the utilization of photoetched grid patterns. The dish structure supporting the grids is rf transparent, requiring the utilization of fiberglass or Kevlar composite construction. Some designs have utilized polarized systems with mechanically overlapping orthogonally polarized reflectors fed by separate feeds to take maximum advantage of the available space on the spacecraft structure.

The spacecraft system requirement for lightweight construction has placed a premium on optimum reflector structural design. When combined with the requirement for stability in the space thermal environment, the trend has been to utilize advanced composite materials, such as graphite and Kevlar fibers supported in an epoxy binder. Three classical reflector configurations have emerged and include (shown in Fig. 1): 1) thick sandwich unstiffened shell, 2) truss-supported thin membrane shell, and 3) rib-stiffened thin sandwich shell. The requirements for precision contours have resulted in the utilization of explicit or implicit postfabrication shape adjustment concepts with each of these reflector configurations. Postfabrication contour adjustment has proven to be a cost-effective technique for fabrication of high-quality reflectors. Rms deviations from a perfect parabola may be reduced by almost one order of magnitude, utilizing adjustments performed during the final reflector assembly.

The thermal control techniques utilized with the various reflector designs for minimizing thermal gradients include thermal coatings, thermal blankets, and thermal shields. The complexity of the spacecraft/reflector configurations requires that a number of standard solar orientations be investigated, such as (see Fig. 2): front sun; side sun; back sun; half-

Presented as Paper 78-593 at the AIAA 7th Communications Satellite Systems Conference, San Diego, Calif., April 24-27, 1978; submitted July 7, 1978; revision received June 25, 1979. Copyright © American Institute of Aeronautics and Astronautics, Inc., 1978. All rights reserved. Reprints of this article may be ordered from AIAA Special Publications, 1290 Avenue of the Americas, New York, N.Y. 10019. Order by Article No. at top of page. Member price \$2.00 each, nonmember, \$3.00 each. **Remittance must accompany order.**

Index categories: Spacecraft Configurational and Structural Design (including Loads); Spacecraft Systems; Structural Composite Materials.

*Assistant Manager, Mechanical Engineering Laboratory, Space Systems Division.

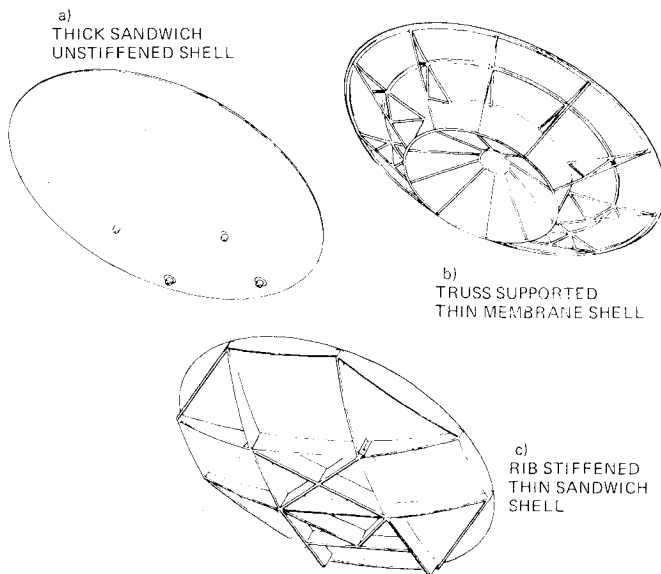


Fig. 1 Classical reflector configurations.

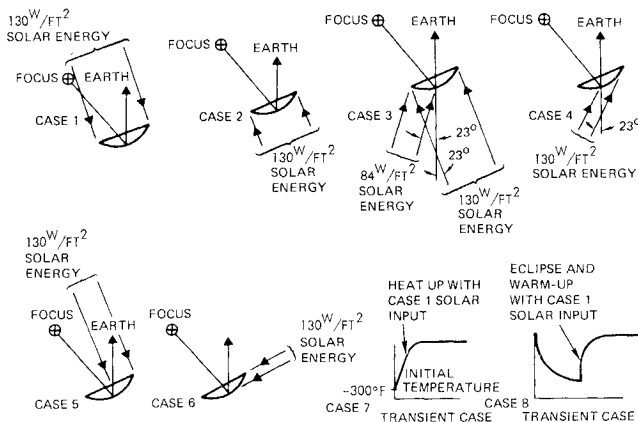


Fig. 2 Typical solar heating cases.

shadowed front sun; eclipse, and eclipse transients. A good system tradeoff has been determined to consist of front face white paint combined with a lightweight thermal blanket on the back face to increase the effective thermal capacitance. The long design life (i.e., 10 years) for communication spacecraft operation requires the use of end-of-life thermal paint properties which are significantly deteriorated compared to beginning-of-life properties. This has caused major problems by requiring composite reflectors to operate at temperatures greater than 200°F.

Error Parameters

Typical parabolic reflector geometry is illustrated in Fig. 3 for axisymmetric and off-axis antenna configurations. The principal parameters in defining the reflector geometry are the focal length of the parabola F , the reflector envelope such as the diameter D , the location of the parabola focal point, and the position of the principal axis of the parabola which passes through the focal point and the parabola vertex.

To function properly as an antenna reflector, the parabola must be properly positioned with respect to the antenna axis and the antenna feed phase center, as shown in Fig. 4, for the more general case of an off-axis configuration. If not properly located, the antenna will not perform in an acceptable manner. The critical errors consist of linear deviation of the reflector focal point from the antenna feed location and angular deviation of the paraboloid principal axis relative to

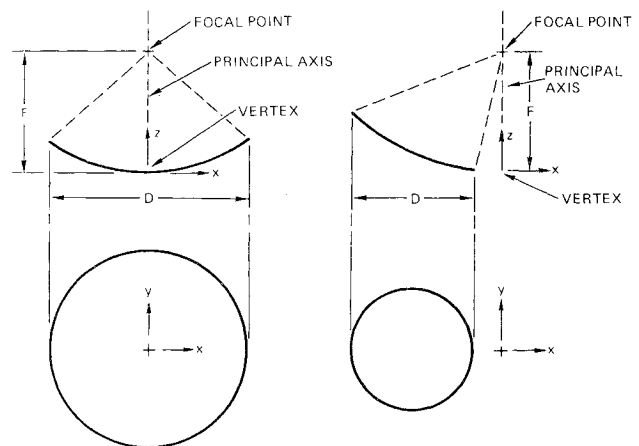
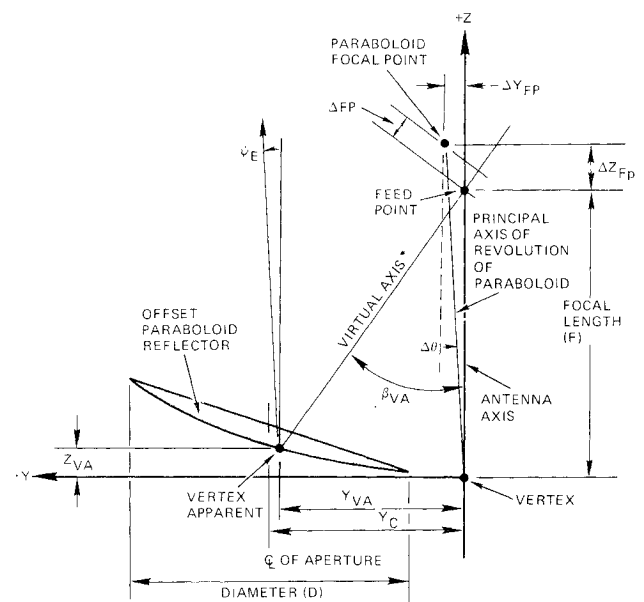


Fig. 3 Paraboloid reflector geometry.



*VIRTUAL AXIS BISECTS ANGLE FROM FEED POINT INTERCEPTED BY REFLECTOR

$$\psi_E = \left(\frac{K}{F + Z_{VA}} \right) (\Delta Z_{FP} \sin \beta_{VA} + \Delta Y_{FP} \cos \beta_{VA}) \frac{180}{\pi} + \Delta \theta$$

$$\Delta F_P = \Delta Z_{FP} \cos \beta_{VA} - \Delta Y_{FP} \sin \beta_{VA}$$

Fig. 4 General paraboloid reflector error geometry.

the antenna axis. This causes a net pointing error in the rf-axis and a defocus of the antenna system.

Additional errors in the reflector performance are caused by deviations of the reflecting surface contour from the ideal parabolic geometry. These deviations result from manufacturing process tolerances and errors, from materials creep or shrinkage, and from environmental extremes in the operational mode. The principal effect of these errors is to contribute to the errors in the focal point location and the paraboloid axis position, and to cause a significant roughness of the surface contour. The magnitude of these errors is quantitatively determined by statistically calculating the best-fit-parabola (BFP) which defines the average contour. The BFP paraboloid is defined as having the least sum-of-squares deviation between the theoretically perfect paraboloid and the data points (measured or analytical) describing the reflector contour. The magnitude of the contour deviation error is defined as the root-mean-square (rms) of the half-path length errors seen by the rf energies focused by the reflector.

The three principal mechanical error parameters to be minimized in order to optimize the performance of an antenna system thus consist of:

- 1) *Pointing*. Minimize the deviation of the electrical boresight with respect to the design antenna pointing axis.
- 2) *Defocus*. Minimize the deviation of the reflector focal point with respect to the antenna feed phase center or equivalent feed location.
- 3) *Contour BFP half-pathlength rms*. Minimize the rms deviation of the reflector contour relative to a mathematically perfect parabola.

Antenna Performance Requirements

The primary antenna performance requirements are related to maximum on-axis gain and antenna beam pointing. Antenna gain is a measure of the maximum signal intensity which is transmitted or received by the antenna from a standard source. The relationship of antenna gain loss, expressed in decibels (dB), to the reflector contour rms was worked out by Ruze¹ for reasonable tolerance losses and for error correlation intervals which are large compared to a wavelength.

The loss ratio is expressed as

$$G/G_0 = \exp \left[- (4\pi\epsilon/\lambda)^2 \right]$$

where ϵ is the rms surface error in the same units as the wavelength λ , G_0 is the antenna gain with a perfect reflector contour, and G is the actual antenna gain. This relationship is plotted in Fig. 5, where it is seen that the detrimental effect of the rms surface error is proportional to the rf frequency at which the antenna operates. Nominally, the maximum acceptable gain loss due to rms surface error is 0.25 dB, which corresponds to an rms value of 0.02λ . Freeland² uses a 0.6 dB gain loss to relate frequency to surface accuracy which corresponds to an rms requirement of 0.03λ .

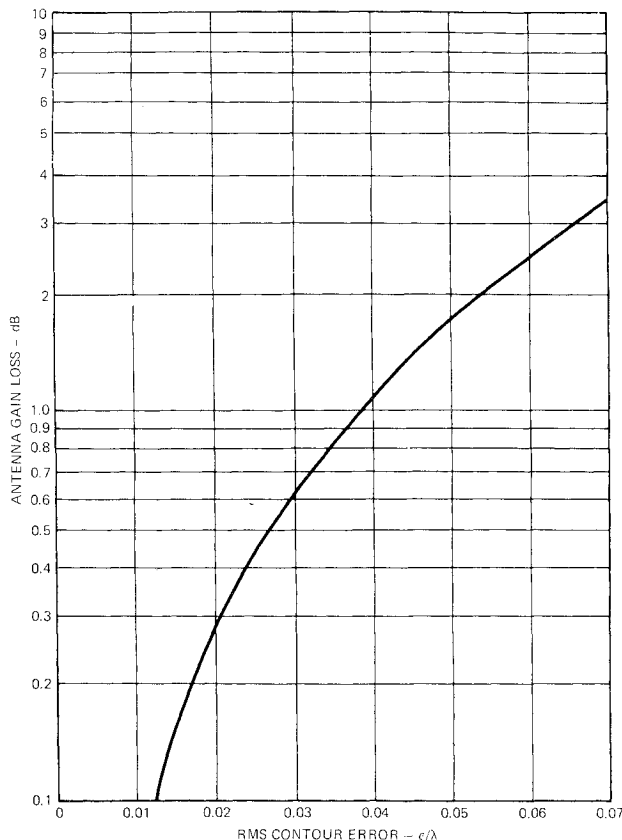


Fig. 5 Gain loss vs reflector contour rms.

The defocus error adversely affects gain and also contributes to the pointing error, as illustrated in Fig. 4, for off-axis configurations. The sensitivity of gain loss to defocus error is less pronounced than for the rms error and has not been modeled parametrically, as was accomplished by Ruze for the contour roughness. If examined simply as an equivalent rms surface deviation from a BFP with focal point located at the fixed-feed phase center, one can rationalize that the defocus error is an order of magnitude ($\times 10^{-1}$) less important than the rms error with respect to gain degradation. The effect of defocus on pointing, however, varies with the antenna configuration geometry and must be examined on an individual basis.

Pointing requirements vary with the rf frequency at which the antenna is operated and are also affected by the nature in which the antenna is operated (i.e., open- vs closed-loop pointing). The basic pointing requirement is related to the half-power beam width which varies with frequency and aperture, as per the following relation for a circular aperture with a parabolic tapered feed illumination³:

$$\theta_H = 1.273 \lambda/D \text{ rad}$$

where λ is the wavelength and D is the diameter of the circular aperture.

Nominal pointing requirements to attain maximum gain may be one-quarter of the half-power beam width. This would result in less than 5% gain loss. Only a portion of this requirement may be allocated to reflector performance, however, resulting in a reflector pointing requirement of one-fifth to one-tenth of the half-power beam width.

In summary, then, the following are nominal requirements for antenna reflector design:

$$\begin{aligned} \text{rms:} &< 0.02\text{--}0.03 \lambda \\ \text{Defocus:} &< 0.2 \lambda \\ \text{Pointing:} &< 10\lambda/D \text{ deg} \end{aligned}$$

Typical Mechanical Requirements

The spacecraft antenna system requirements are normally stated in terms of rf performance. When implemented for the antenna structure subsystem, the requirements are stated in terms of mechanical requirements, such as stiffness, strength, temperature, thermoelastic distortions, weight, and manufactured contour accuracy. Typical mechanical requirements for a large off-axis reflector, for example, might be summarized as follows:

- 1) *Stiffness*. Stowed, the fundamental vibration frequency should exceed 20 Hz; deployed, the fundamental vibration frequency should exceed 10 Hz.
- 2) *Strength*. This requirement varies with unit weight of reflector and direction of load application. For a high unit weight, the limit load factor may be 10 g in all directions, whereas for a low unit weight, the limit load factor may be 15-25 g in all directions to account for increased sensitivity to acoustic excitation.
- 3) *Temperature*. This requirement, if any, is a function of the materials of which the unit is constructed. For currently used composite materials, the maximum environmental exposure should not exceed about 200°F.
- 4) *Thermoelastic distortions*. It is convenient from a mechanical point of view to base the contour shape requirements on a statistical best-fit-paraboloid (BFP) analysis. The specific requirements are a function of the operational rf frequency. For a C-band system operating at 4 and 6 GHz, the allowable BFP focal length change may be ± 0.200 in., the random deviation from a perfect paraboloid contour should not exceed 0.010 in. rms, and the electrical boresite shift should not exceed 0.05 deg based on the BFP analysis. These allowances may be defined to include

deviations from all causes, such as manufacturing, handling and test, boost environment, and orbital environment.

5) *Manufactured contour accuracy.* The manufactured contour accuracy is also specified based on a BFP analysis. These requirements are a function of the operational rf frequency. For a C-band system operating at 4 and 6 GHz, the deviation in the BFP focal point location of the assembled reflector should not exceed ± 0.100 in., and the random deviation from a perfect paraboloid contour should not exceed 0.015 in. rms (when combined with the orbital distortions, this results in a net 0.018 in. rms). The reflector mechanical boresite of the assembled reflector should not deviate more than 0.05 deg from the nominal position.

6) *Weight.* The allowable unit weight is a function of the size and method of attachment, but generally is required to be less than 0.5 psf of reflector aperture area.

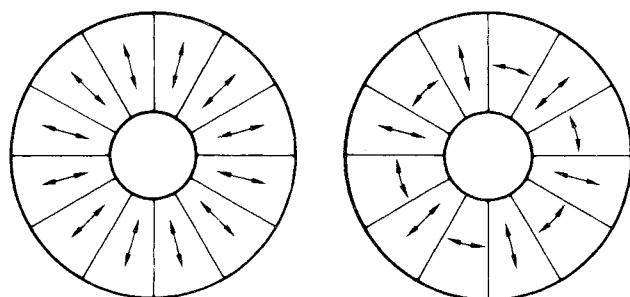
Performance Prediction

Contour Distortion

The development of high-performance parabolic antenna reflectors to meet high standards of performance has led to the utilization of advanced composite materials to provide the required thermoelastic stability in the space environment and to maintain a suitable lightweight configuration. For example, the requirements just specified for a large off-axis reflector require utilization of a structural material with a thermal expansion coefficient less than $0.5 \times 10^{-6}/^{\circ}\text{F}$. This performance can be provided by utilization of a graphite or Kevlar fiber-reinforced epoxy construction.

Analysis of the mechanical performance of a composite structure design requires evaluation of several factors which are normally considered secondary and insignificant in conventional homogenous materials. Consider that an "isotropic" composite layup, designed with a low thermal expansion coefficient, may deviate by $0.1\text{--}0.2 \times 10^{-6}/^{\circ}\text{F}$ between the orthogonal principal axes of the layup due to subtleties in the design configuration. This "insignificant" deviation would normally be of only slight importance. However, if the average "isotropic" thermal expansion value is $0.2 \times 10^{-6}/^{\circ}\text{F}$, then the associated anisotropic characteristic assumes a first-order importance and must be included in the analysis. Similarly, material and process tolerances in composite material layups may result in deviations from the nominal of 25-50% in the near-zero average "isotropic" expansion coefficient. The effect of this deviation in properties must be evaluated for possible differences in front vs back reflector structure average thermal expansion, and may be of first-order importance in the distortion analysis. It has been observed that off-axis paraboloid reflectors may be more sensitive to the anisotropic material characteristics than to the average "isotropic" behavior.

A similar sensitivity to anisotropic material effects has also been observed for large axisymmetrical paraboloidal reflectors. Consider a symmetrical "isotropic" composite



a. RADIALLY CORRELATED DIFFERENTIAL THERMAL EXPANSION

b. AVERAGED DIFFERENTIAL THERMAL EXPANSION

Fig. 6 Plan view of symmetrical reflector construction.

material configuration with a differential thermal expansion, which is correlated with the radial and tangential directions in the paraboloidal shell. A differential of $0.2 \times 10^{-6}/^{\circ}\text{F}$ compared with an average "isotropic" value of 0.5×10^{-6} per $^{\circ}\text{F}$ has been observed to have a first-order effect on thermal distortions. This has resulted in the development of design configurations which attempt to reduce to zero the effective correlated differential expansion (see Fig. 6). In addition, material processes are optimized to minimize the effective differential effects which result from honeycomb core orientation, composite woven cloth "warp" vs "woof" differences, and double-curvature shell effects which distort the relative fiber angles in oriented layups.

Other effects observed in the behavior of composite materials which affect the reflector contour distortion include shrinkage due to loss of moisture in the space environment and variation in thermal expansion with exposure to the orbital thermal extremes. It has been observed that graphite-fiber reinforced epoxies (GFRE) may shrink by $0.01 \pm 0.005\%$ over a period of days to weeks due to loss of moisture in the space environment. This leads to a test requirement that the reflector contour shape and alignment be established in a low-humidity environment to reasonably simulate the dry space environment.

Long-term aging effects in the space environment have been simulated by subjecting small coupons to cyclic temperature extremes in a vacuum environment. These tests on "isotropic" composite configurations have consistently resulted in thermal expansion coefficients becoming more negative by $0.15\text{--}0.25 \times 10^{-6}/^{\circ}\text{F}$ after 1000-10,000 cycles of exposure to temperatures between -250 and $+150^{\circ}\text{F}$ (see Fig. 7). This effect is accounted for in evaluating the end-of-life behavior in high-performance reflectors.

Temperature

The use of composites and sandwich construction requires careful attention to thermal control to maintain reasonable minimum and maximum temperature limits, which are compatible with the materials and adhesives of which the structure is fabricated. Normal space exposure with white painted surfaces supplemented with backside thermal blankets will result in temperatures from -300°F to about $+180^{\circ}\text{F}$ at synchronous altitude. However, the effect of ir radiation and specular reflection from the spacecraft structure may increase temperatures locally above 200°F on the

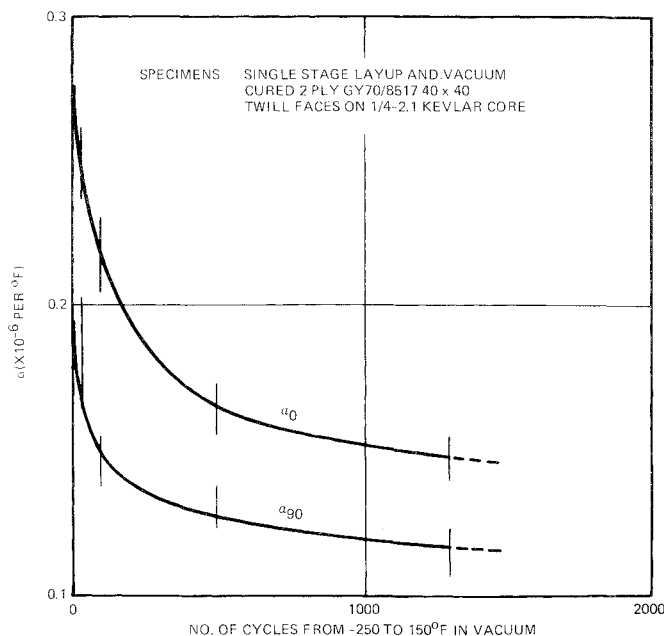


Fig. 7 Typical effect of thermal cycling on thermal expansion.

reflector (see Fig. 2). In addition, the effect of sun focusing on the spacecraft feed and feed support structures at some orientations will require special treatment of the spacecraft to avoid runaway temperature situations. Practically speaking, feed structures are very vulnerable to "solar boiler" heating from large solid parabolic reflectors with surfaces whose specularly may range from 0.1 to larger than 1%.

Thermal coatings and paints, which are compatible with the low thermal expansion composite surfaces in extreme environments, are difficult to find. Many deleterious phenomena have been observed with painted composite surfaces at very low temperatures, such as "dandruff" (a powdering deterioration of the paint), cracking of the paint surface, peeling in which the composite laminate is damaged, and modification of the effective structure thermal stability due to "change of state" in the paint material at low temperatures. In order to avoid these problems, one is forced to utilize coatings with less than optimum thermal properties, or to avoid using any thermal coatings.

Reflector Manufactured Performance

Nondeployable solid contour reflectors for spacecraft applications vary from 1-12 ft in diameter. Reflectors larger than about 12 ft in diameter exceed the dynamic envelope of existing booster shrouds or the shuttle cargo bay, and must be folded or, otherwise, stowed for launch. These reflectors have been fabricated successfully of various materials, including aluminum, fiberglass, Kevlar, and graphite-fiber reinforced epoxy (GFRE). Three different configurations based on external envelopes are considered here. These consist of: 1) a thick sandwich shell with structural facesheets supported by a honeycomb core with a central attachment fitting; 2) a thin sandwich shell stiffened by a network of supporting ribs which attach to the supporting structure; and 3) a thick sandwich shell with an adjustable circular stiffening ring attached adjacent to the shell periphery and having a centrally located supporting structure.

The mechanical errors which affect the performance in orbit result from several sources, including the manufacturing process, assembly tolerances, test and launch environments, thermal environments in orbit, and material aging effects. In general, the effects of test and launch environments, thermal environments in orbit, and material aging effects are controlled by the designer in his selection of the design configuration and materials of construction. We are primarily concerned here with the errors resulting from the manufacturing and assembly of the reflector with the antenna subsystem.

An important distinction may now be observed with respect to the relative significance of rms errors, defocus errors, and pointing errors which occur during the reflector manufacturing process, as follows: If adequate adjustment capability is provided in the design of the antenna assembly, defocus and pointing errors may be effectively eliminated in the assembled system, limited only by the capability and tolerances of the assembly/test equipment. The only significant residual error at the beginning-of-life for a nondeployable solid contour reflector is thus the contour rms.

The manufactured rms performance of approximately 100 nondeployable spacecraft reflectors from 2 to 9 ft in diameter fabricated over a period of 12 years is summarized in Table 1. The rms error is normalized to the diameter for a circular aperture or by the greatest lateral dimension for a noncircular aperture. It is thus assumed, for a particular configuration and material, that the manufactured rms error will vary directly as the size of the reflector. On this basis, a correlation has been accomplished for the various design configurations, materials, and manufacturing processes.

It is evident from the correlation summary that the manufactured rms performance of reflectors fabricated from aluminum and GFRE materials is considerably better than for

Table 1 Nondeployable reflector performance correlation

Material	Configuration	Normalized contour rms (δ/D)
Fiberglass	Sandwich shell	$> 5 \times 10^{-4}$
	Adjusted shell	0.7×10^{-4}
Kevlar	Rib-supported shell	0.6×10^{-4}
Aluminum	Sandwich shell	0.5×10^{-4}
GFRE	Sandwich shell	0.9×10^{-4}
	Rib-supported shell	0.3×10^{-4}
	Adjusted shell	0.14×10^{-4}

those fabricated from fiberglass and Kevlar materials. This is probably related to the elastic modulus of the construction materials; the higher the modulus and the stiffer the reflector the better the contour rms. It is also observed that configurations which incorporate a postfabrication adjustment concept have a significantly improved rms performance.

All of the reflectors included in the preceding study were fabricated utilizing conventional metallic layup molds with a surface contour precise to 0.001 in. rms or better.

It is observed from Table 1 that considerable improvement in the manufactured rms of a rigid reflector is achieved by incorporating an adjustment feature in the reflector design, which provides capability for contour adjustment following fabrication of the reflector structure. An rms improvement factor of 5 has been realized in specific designs by this technique. In addition to improving the contour rms, the reflector shape is also stabilized against long-term changes due to creep and the reflector structure is rigidized. Similar characteristics are provided, although in a less explicit manner, by the rib structure in the rib-stiffened shell configuration, as will be discussed. It is observed that this design also provides a significant improvement by a factor of 3 in the contour rms, compared to the nonstiffened shell configuration.

The nominal manufacturing flow utilized in the fabrication of the rib-stiffened shell configuration provides for fabrication of the shell and ribs independently. Subsequently, the shell contour is firmly supported on the layup mold, while the unstressed ribs are permanently bonded to the shell to stiffen and stabilize the reflector. An implicit postfabrication shaping is thus accomplished for the shell contour in the final assembly process, which results in major shape improvement. GFRE reflectors 5 ft in diameter have thus been fabricated which have contour rms tolerances from 0.0012 to 0.0027 in., corresponding to an average $\delta/D = 0.3 \times 10^{-4}$. The success of this technique depends upon: 1) the precision of the layup mold; 2) the use of rigid ribs located close to the shell periphery, and 3) the avoidance of initial stresses in the supporting rib structure during the assembly bonding operation. This design approach has been successfully utilized to provide lightweight, rigid, and thermally stable reflectors for the Satcom, Anik B, and Intelsat V communication spacecraft.

Figure 8 illustrates a parabolic reflector design that incorporates a peripherally located stiffening ring feature which provides a mechanism for explicit postfabrication adjustment of the reflector contour to improve the manufactured rms performance. The stiffening ring is attached to the back edge of the reflector shell by adjustable support brackets. The support brackets are rigidly attached to the reflector shell and are spaced sufficiently close to simulate a continuous reaction. By careful adjustment of the relative distance between the shell and the stiffening ring, the shell contour can be varied by small but significant amounts and a major improvement in contour precision achieved by removing the primary $\cos 2\theta$ distortion in the shell structure. The circular

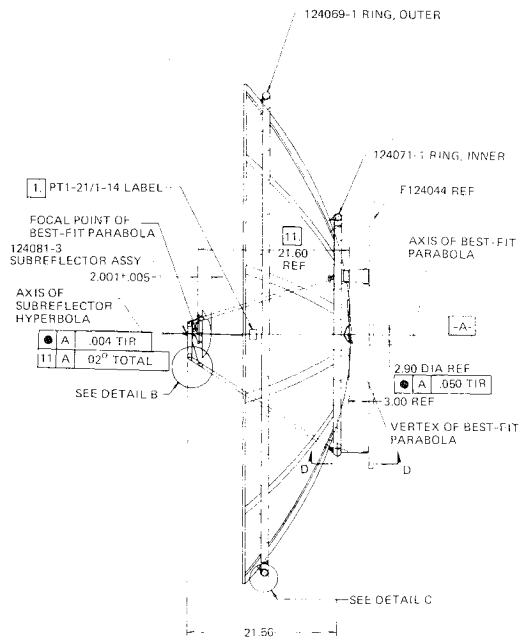


Fig. 8 Reflector configuration with adjustable stiffening ring.

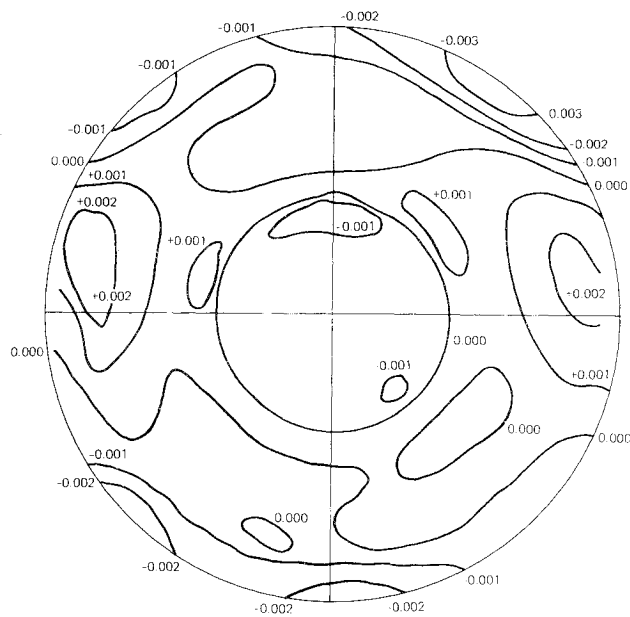


Fig. 9 Contour plot for adjusted shape of 6-ft reflector.

geometry of axisymmetric paraboloids, with which this adjustable stiffening ring technique is used, has resulted in the development of techniques for very rapid optimization of the contour shape simultaneous with the contour measurement for flight hardware. Typically, a 0.001 in. rms is achieved for a 6-ft diameter GFRE reflector. A contour of the final adjusted shape is shown in Fig. 9 based on a BFP analysis.

This design approach for a peripheral stiffening ring is also feasible for off-axis paraboloidal reflectors with a circular projected aperture. In this case, the edge of the reflector has an elliptical shape, and lies in a plane canted to the antenna axis. Similarly, the adjustable stiffening ring would be elliptical and planar, and could be readily adjusted to optimize the reflector contour. In contrast, the reflector edge for a noncircular projected aperture is not planar and, in general, would require a nonplanar noncircular peripheral stiffening structure for adjustment. For example, an egg-crate rib structure has been proposed as the peripheral stiff-

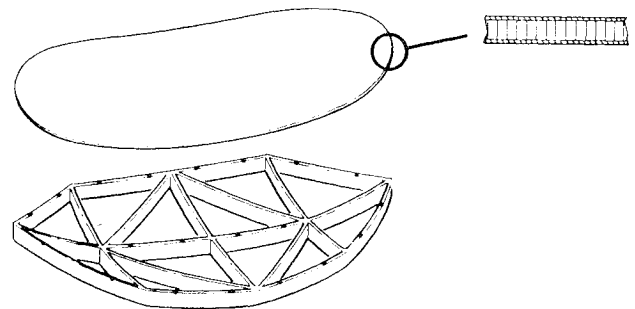
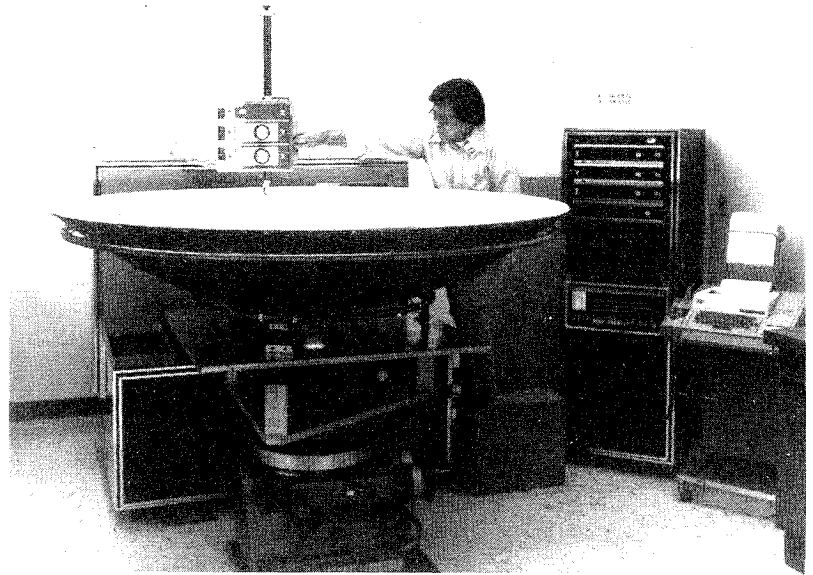


Fig. 10 Reflector stiffening rib design for contour adjustment.

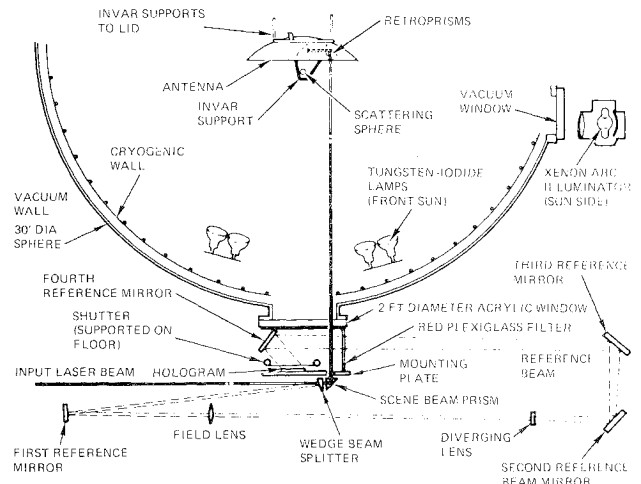


Fig. 11 Distortion measurement by holographic interferometric technique.

ening/adjustment structure for an elliptical off-axis reflector, as shown in Fig. 10.

For thermal stability, the stiffening ring thermal expansion must be compatible with the reflector primary structure material. Thus, aluminum stiffening rings have been used with fiberglass and aluminum reflectors, invar stiffening rings with GFRE reflectors, and GFRE stiffening rib structures with GFRE reflectors.

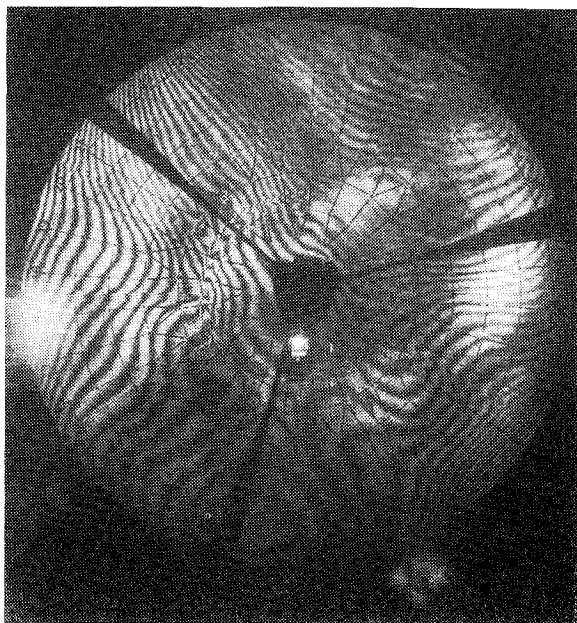


Fig. 12 Typical interferogram of thermally distorted contour.

The full potential for precision nondeployable reflector fabrication using the postfabrication adjustment technique has yet to be realized. The results just quoted have been achieved using conventional tooling with nominal contour accuracy of 0.001 in. rms. The use of precision tooling with a contour rms of 0.0002 in. would provide a capability for GFRE reflectors with a normalized rms contour precision of $\delta/D = 0.7 \times 10^{-5}$, compared to the present performance of $\delta/D = 1.4 \times 10^{-5}$.

Verification

Verification of reflector contour stability in a thermal vacuum environment is an area of extreme difficulty. The primary verification is classically based on analytical evaluations, utilizing material properties obtained from coupon tests. All-up mechanical performance verification has been accomplished by observing the behavior of a very limited number of contour points using techniques ranging from

conventional to exotic, which hopefully are representative of the general structural behavior. A more satisfactory verification of the complete contour behavior has been accomplished using photogrammetric and holographic techniques. The photogrammetric⁴ technique has been standardized and utilized in numerous instances. The holographic technique has had only limited utilization for situations requiring high-precision measurements (see Figs. 11 and 12). The current practice is to place primary reliance on analysis.

Quality control is provided primarily by coupon test procedures. Nondestructive test techniques are also utilized, but less frequently due to technical limitations and high cost for establishing standards on a small number of units.

Conclusion

The design and fabrication of high-precision parabolic reflectors for high-performance antenna systems has required the development of new materials, advanced analysis techniques, new considerations for thermal control, sophisticated verification testing, and designs which employ cost-effective manufacturing processes. Some problems, such as solar heating of the feed structure or deterioration of performance with age, cannot always be solved by changing the reflector configuration, and may seriously compromise the system design. Over the years, many surprises have been encountered which have required close coordination between engineering, materials, manufacturing, and test personnel to develop optimum designs. Considering the many secondary effects which have become of first-order importance in the current state of the art, it is the writer's opinion that further improvements in spacecraft reflector performance will only be attained at greatly increased costs.

References

- ¹Ruze, J., "Antenna Tolerance Theory," *Proceedings of the IEEE*, Vol. 54, April 1966, pp. 633-640.
- ²Freeland, R. E., "Industry Capability for Large Space Antenna Structures," JPL Rept. 710-12, May 1978.
- ³Bathker, D. A. (ed.), "Microwave Performance Characterization of Large Space Antennas," JPL Publication 77-21, May 1977.
- ⁴*Space Chamber Photogrammetry Is Here*, DBA Systems Inc., Melbourne, Fla., 1975.